

Some Statistic and Information-theoretic Results on Arithmetic Average Density Fusion

Tiancheng Li, Yue Xin, Yan Song, Enbin Song and Hongqi Fan

Abstract—Finite mixture such as the Gaussian mixture is a flexible and powerful probabilistic modeling tool for representing the multimodal distribution widely involved in many estimation and learning problems. The core of it is representing the target distribution by the *arithmetic average* (AA) of a finite number of sub-distributions which constitute the mixture. The AA fusion has demonstrated compelling performance for both single-sensor and multi-sensor estimator design. In this paper, some statistic and information-theoretic results are given on the AA fusion approach, including its covariance consistency, mean square error, mode-preservation capacity, mixture information divergence and principles for fusing/mixing weight design. In particular, based on the concept of *conservative fusion*, the relationship of the AA fusion with the existing conservative fusion approaches such as *covariance union* and *covariance intersection* is exposed. The best fit of the mixture is formulated as a max-min problem, proving the sub-optimality of the AA fusion. Linear Gaussian models are considered for illustration and simulation comparison.

Index Terms—Finite mixture, conservative fusion, arithmetic average, linear fusion, covariance intersection, covariance union.

I. INTRODUCTION

THE last two decades have witnessed a steady uptick in the application of the linear information fusion approach such as the averaging operation to the state estimation problem [1]–[4]. Two common types of estimator information that need to be averaged are variables and probability distributions/functions. They correspond to the two classes of estimators: the point estimator such as the most known Kalman filter of which the estimate is given in terms of a point estimate associated with covariance and the density estimator such as the particle filter of which the estimate is given in terms of the Bayesian posterior density. Both types of fusion has seen substantial interest for multi-agent collaboration thanks to the vitalization of networked sensors/systems [2]–[5]. However, the average of variables is a variable of compelling statistical property [6] while the average of distributions is a finite mixture distribution (FMD). In the FMD, mixands are properly weighted and correspond to the information gained from

different fusing sources. They jointly approximate the target distribution $p(\mathbf{X})$ by their arithmetic average (AA):

$$f_{AA}(\mathbf{X}) := \sum_{i \in \mathcal{I}} w_i f_i(\mathbf{X}), \quad (1)$$

where \mathbf{X} stands for the state of a single or multiple target(s), $\mathbf{w} := [w_1, w_2, \dots, w_I]^T$ are positive, normalized mixing/fusing weights, and $f_i(\mathbf{X})$ are the probability distributions (of the same family or not), e.g., probability density function (PDF) and probability hypothesis density function [7], yielded by a finite set of estimators $i \in \mathcal{I} = \{1, 2, \dots, I\}$ conditioned on different observation, models or hypotheses.

The linear AA fusion has provided a compelling approach to multi-sensor random set information fusion [8]–[16], which enjoys high efficiency in computation, tolerance to sensor fault (such as misdetection), and insensitivity to internode correlation. In fact, the need for FMD may also arise in the single-sensor setup due to stochastically switched models of the real state [17], [18], multi-modal data/noise [19], [20] and multiple objects [7], [21]. FMD facilitates the recursive Markov-Bayesian filtering calculation greatly in two means: First, a mixture of conjugate priors is also conjugate and can approximate any kind of prior [22], [23]. Second, the linear fusion of a finite number of mixtures of the same parametric family remains a mixture of the same family. These properties play a key role in the mixture filters such as the Gaussian mixture (GM) filter, Student's- t mixture filter [24] and multi-Bernoulli mixture filters [7], [25], [26]. In fact, FMD has also been widely used in machine learning [27].

Nevertheless, theoretical study on the AA density fusion approach is still short in two aspects. First, while the concept of conservative fusion has been well accepted, the AA fusion gains the above mentioned advantages at the price of an inflated covariance which seems at variant with the minimum variance estimator/fusion. This unavoidably raises a concern on the accuracy of the estimator if one simply swaps the inflated variance with increased mean square error (MSE). We in this paper clarify their fundamental difference and provide an in-depth analysis of the statistics of the AA fusion and its connection with existing conservative fusion approaches. Second, while AA-fusion/FMD has proven successful in practice, it remains unclear how the mixture as a whole compares with the mixands (especially the *best* one) and how the fusing weights should be designed in order to maximize the fusion gain if there is any. We provide information-theoretic results to answer these questions. These original statistic and information-theoretic findings are expected to underpin the use of the FMD and AA fusion approach.

Manuscript preprint

This work was partially supported by National Natural Science Foundation of China under grant 62071389 and by the Key Laboratory Foundation of National Defence Technology (JKWATR-210504).

T. Li, Y. Xin and Y. Song are with the Key Laboratory of Information Fusion Technology (Ministry of Education), School of Automation, Northwestern Polytechnical University, Xi'an 710129, China, e-mail: t.c.li@nwpu.edu.cn

E. Song is with the College of Mathematics, Sichuan University, Chengdu, China, e-mail: e.b.song@163.com

H. Fan is with the Key Laboratory of Science and Technology on ATR, National University of Defense Technology, Changsha 410073, Hunan, China. E-mail: fanhongqi@nudt.edu.cn

The remainder of this paper is organized as follows. In section II, we analyze and compare several classic conservative estimation approaches, highlighting the fault-tolerance and mode-preservation feature of the AA fusion approach. In section III, we study the exact divergence of the mixture from the true/target distribution, providing an information-theoretic justification for the AA fusion. Then, we propose approaches to fusing weight design. Simulation study is presented in section IV. We conclude the paper in section V.

II. CONSERVATIVE FUSION AND STATISTICS OF AA

In the context of time-series estimation, optimality is usually sought such as minimum MSE (MMSE) and minimized Bayes risk [28], resulting in different classes of estimators: MMSE point estimator and Bayes-optimal density estimator. There is a key difference between two optimal criterion: the former relies on the statistics of the estimator such as the mean and variance, and the latter on the quality of the posterior for which a proper distribution-oriented metric such as the Kullback Leibler (KL) divergence is useful.

The very nature of optimal fusion in the sense of whether MMSE or Bayes needs to quantify the exact cross-correlation among the information sources [29], [30]. Unfortunately, this often turns out to be impractical due to the complicated, ubiquitous, latent correlation among sensors/agents and so one has to resort to suboptimal, correlation-insensitive solutions such as the AA fusion.

A. Notations, Concepts and Definitions

Note that the mean of the multitarget distribution corresponds to the state of no target while the variance relies on not only the estimation uncertainty but also on the distance among targets. Therefore, statistics such as the mean and variance do not apply to the multi-target estimator. In this section, we limit statistics analysis with respect to a single target only.

In the following, we use $\mathbf{x} \in \mathbb{R}^{n_x}$ to denote the n_x -dimensional state of the target which is a random quantity to be estimated, namely the true state. We use $p(\mathbf{x})$ to denote the corresponding PDF, namely the true distribution of \mathbf{x} . For a given Bayesian posterior $f(\mathbf{x})$ which is an estimate to the real distribution $p(\mathbf{x})$ conditioned on some observations¹, from which the state estimate can be attained in either of two common ways, namely the expected a posteriori (EAP) and maximum a posteriori (MAP) estimators as follows

$$\hat{\mathbf{x}}^{\text{EAP}} = \int_{\mathbb{R}^{n_x}} \tilde{\mathbf{x}} f(\tilde{\mathbf{x}}) d\tilde{\mathbf{x}}, \quad (2)$$

$$\hat{\mathbf{x}}^{\text{MAP}} = \arg \sup_{\tilde{\mathbf{x}} \in \mathbb{R}^{n_x}} f(\tilde{\mathbf{x}}). \quad (3)$$

That is, in the EAP estimator, the state estimate is given as the mean of the posterior while in the MAP the state estimate is given as the peak/mode of the posterior distribution.

We consider a number of estimate pairs, each composed of a state estimate $\hat{\mathbf{x}}_i$ and an associated positive-definite error covariance matrix \mathbf{P}_i , $i \in \mathcal{I}$, which are to be fused using

¹Hereafter, we ignore the dependence on those random observations for simplicity unless when the random nature of the posterior is addressed.

weights $\mathbf{w} := \{w_1, w_2, \dots, w_I\}$, where $w_i > 0$, $\mathbf{w}^T \mathbf{1}_I = 1$. Hereafter, $\hat{\mathbf{x}}_i$ is given by the EAP estimator unless otherwise stated. Then, each estimate pair corresponds to the first and second moments of the posterior PDF $f_i(\mathbf{x})$ that is an estimate of the true distribution $p(\mathbf{x})$, i.e., $\hat{\mathbf{x}}_i = \int_{\mathbb{R}^{n_x}} \tilde{\mathbf{x}} f_i(\tilde{\mathbf{x}}) d\tilde{\mathbf{x}}$, $\mathbf{P}_i = \int_{\mathbb{R}^{n_x}} (\tilde{\mathbf{x}} - \hat{\mathbf{x}}_i)(\cdot)^T f_i(\tilde{\mathbf{x}}) d\tilde{\mathbf{x}}$ ². Hereafter, we use the shorthand writing $(\mathbf{x} - \mathbf{y})(\cdot)^T$ for representing $(\mathbf{x} - \mathbf{y})(\mathbf{x} - \mathbf{y})^T$. The MSE of $\hat{\mathbf{x}}_i$ is denoted as

$$\text{MSE}_{\hat{\mathbf{x}}_i} := \mathbb{E}[(\mathbf{x} - \hat{\mathbf{x}}_i)(\cdot)^T] = \int_{\mathbb{R}^{n_x}} (\tilde{\mathbf{x}} - \hat{\mathbf{x}}_i)(\cdot)^T p(\tilde{\mathbf{x}}) d\tilde{\mathbf{x}}.$$

Definition 1 (conservative). An estimate pair $(\hat{\mathbf{x}}, \mathbf{P}_{\hat{\mathbf{x}}})$ regarding the real state \mathbf{x} , is deemed conservative [31]–[34] when

$$\mathbf{P}_{\hat{\mathbf{x}}} \succeq \text{MSE}_{\hat{\mathbf{x}}}. \quad (4)$$

That is, $\mathbf{P}_{\hat{\mathbf{x}}} - \mathbb{E}[(\mathbf{x} - \hat{\mathbf{x}})(\cdot)^T]$ is positive (semi-)definite.

The notion is also referred to as *covariance consistent* and as pessimistic definite [35]. Extended definition of the conservativeness of PDFs can be found in [36], [37]. A relevant notion of “informative” is given as follows

Definition 2 (informative). An estimate pair $(\hat{\mathbf{x}}_1, \mathbf{P}_1)$ is said to be more informative than $(\hat{\mathbf{x}}_2, \mathbf{P}_2)$ regarding the same state \mathbf{x} when $\mathbf{P}_1 \prec \mathbf{P}_2$.

With respect to the type of data, there are two forms of AA fusion as follows.

Definition 3 (AA v-fusion). In a point estimation problem, the AA *v*-fusion is carried out with regard to these state estimate variables $\hat{\mathbf{x}}_i$, $i \in \mathcal{I}$ which yields a new variable

$$\hat{\mathbf{x}}_{\text{AA}} = \sum_{i \in \mathcal{I}} w_i \hat{\mathbf{x}}_i. \quad (5)$$

Definition 4 (AA f-fusion). In the Bayesian formulation, the estimation problem is to find a distribution that best fits $p(\mathbf{x})$. The corresponding AA *f*-fusion is carried out with regard to $f_i(\mathbf{x})$, $i \in \mathcal{I}$ which yields a mixture of these fusing distributions, a FMD

$$f_{\text{AA}}(\mathbf{x}) = \sum_{i \in \mathcal{I}} w_i f_i(\mathbf{x}). \quad (6)$$

B. Conservative Fusion: CU versus AA

Based on the concept of conservativeness, there are a number of results as given in the following Lemmas.

Lemma 1. For a set of estimate pairs $(\hat{\mathbf{x}}_i, \mathbf{P}_i)$, $i \in \mathcal{I}$ in which at least one is conservative, a sufficient condition for the fused estimate pair $(\hat{\mathbf{x}}_{\text{AA}}, \mathbf{P}_{\text{CU}})$ to be conservative is that

$$\mathbf{P}_{\text{CU}} \succeq \mathbf{P}_i + (\hat{\mathbf{x}}_{\text{AA}} - \hat{\mathbf{x}}_i)(\cdot)^T, \quad \forall i \in \mathcal{I}, \quad (7)$$

of which a tight bound is given by³

$$\mathbf{P}_{\text{CU}}^u := \max_{i \in \mathcal{I}} \left(\mathbf{P}_i + (\hat{\mathbf{x}}_{\text{AA}} - \hat{\mathbf{x}}_i)(\cdot)^T \right). \quad (8)$$

²Note that a Gaussian PDF can be uniquely determined by an estimate pair. Fusing in terms of only the mean and variance implicitly imposes Gaussian assumption. These being said, the AA density fusion is by no means limited to any specific distributions or finite moments of the distribution.

³We note that two covariance matrixes may not be comparable for which we use $\mathbf{A} \succ \mathbf{B}$ if $\text{Tr}(\mathbf{A}) > \text{Tr}(\mathbf{B})$, where $\text{Tr}(\mathbf{A})$ calculates the trace (or the determinant) of matrix \mathbf{A} .

Proof for Lemma 1 can be found in [8]. It actually provides a conservative fusion method which is known as covariance union (CU) [32], [38], [39]. It is deemed *fault tolerant* as it preserves covariance consistency as long as at least one fusing estimator is conservative. When all fusing estimators are conservative, i.e., $\mathbf{P}_i \succeq \mathbb{E}[(\mathbf{x} - \hat{\mathbf{x}}_i)(\cdot)^T]$, $\forall i \in \mathcal{I}$, a more informative estimator can be obtained by the following Lemma

Lemma 2. For a set of conservative estimate pairs $(\hat{\mathbf{x}}_i, \mathbf{P}_i)$, $i \in \mathcal{I}$, a sufficient condition for the fused estimate pair $(\hat{\mathbf{x}}_{AA}, \mathbf{P}_{CU}^l)$ to be conservative is given by

$$\mathbf{P}_{CU}^l := \min_{i \in \mathcal{I}} (\mathbf{P}_i + (\hat{\mathbf{x}}_{AA} - \hat{\mathbf{x}}_i)(\cdot)^T). \quad (9)$$

Lemma 3. For Gaussian distributions $f_i(\mathbf{x}) = \mathcal{N}(\mathbf{x}; \hat{\mathbf{x}}_i, \mathbf{P}_i)$ with mean $\hat{\mathbf{x}}_i$ and covariance \mathbf{P}_i , $i \in \mathcal{I}$, the AA f -fusion (6) results in a FMD for which the mean and covariance are respectively given by (5) and

$$\mathbf{P}_{AA} = \sum_{i \in \mathcal{I}} w_i \tilde{\mathbf{P}}_i, \quad (10)$$

where the adjusted covariance matrix is given by

$$\tilde{\mathbf{P}}_i := \mathbf{P}_i + (\hat{\mathbf{x}}_{AA} - \hat{\mathbf{x}}_i)(\cdot)^T. \quad (11)$$

Proof. First, $\hat{\mathbf{x}}_{AA} = \int_{\mathbb{R}^{n_x}} \tilde{\mathbf{x}} \sum_{i \in \mathcal{I}} w_i f_i(\tilde{\mathbf{x}}) d\tilde{\mathbf{x}} = \sum_{i \in \mathcal{I}} w_i \hat{\mathbf{x}}_i$. Proof of (10) for fusing two Gaussian distributions can be found in Appendix B of [15], which can be easily extended to any finite number of fusing distributions. \square

The Appendix B of [15] further showed that, the above results $\hat{\mathbf{x}}_{AA}$ and \mathbf{P}_{AA} correspond to the first and second moments of the resulting Gaussian distribution by merging [40] all mixands in the mixture. In fact, the Gaussian PDF that best fits the AA mixture has the same first and second moments [41, Theorem 2], i.e.,

$$(\hat{\mathbf{x}}_{AA}, \mathbf{P}_{AA}) = \arg \min_{(\mu, \mathbf{P})} D_{KL}(f_{AA} \| \mathcal{N}(\mu, \mathbf{P})), \quad (12)$$

where $D_{KL}(f \| p) := \int_{\mathbb{R}^{n_x}} f(\mathbf{x}) \log \frac{f(\mathbf{x})}{p(\mathbf{x})} d\mathbf{x}$ denotes the KL divergence of the probability distribution $p(\mathbf{x})$ relative to $f(\mathbf{x})$.

According to the expressions (8), (9) and (10), we have a *conservative fusion chain*:

$$\mathbf{P}_{\text{Naive}} \prec \min_{i \in \mathcal{I}} (\mathbf{P}_i) \preceq \mathbf{P}_{CU}^l \preceq \mathbf{P}_{AA} \preceq \mathbf{P}_{CU}^u, \quad (13)$$

where $\min_{i \in \mathcal{I}} (\mathbf{P}_i) = \mathbf{P}_{CU}^l$ holds if and only if (iif) $\hat{\mathbf{x}}_{AA} = \hat{\mathbf{x}}_i$ in (9), $\mathbf{P}_{CU}^l = \mathbf{P}_{AA} = \mathbf{P}_{CU}^u$ holds iff $\tilde{\mathbf{P}}_i = \tilde{\mathbf{P}}_j$, $\forall i \neq j$ and

$$\mathbf{P}_{\text{Naive}} = \left(\sum_{i \in \mathcal{I}} \mathbf{P}_i^{-1} \right)^{-1}, \quad (14)$$

which corresponds to the covariance of the multiplied Gaussian distribution, i.e., $\mathcal{N}(\mu_{\text{Naive}}, \mathbf{P}_{\text{Naive}}) = \prod_{i \in \mathcal{I}} \mathcal{N}(\mu_i, \mathbf{P}_i)$.

The chain (13) implies that the AA fusion trades off between conservative and informative, lying between the two scenario-specific choices corresponding to the following two scenarios: (i) all fusing estimators are conservative and (ii) at least one fusing estimator is conservative.

C. Fusion: More or Less Conservative

In contrast to the AA fusion (6), the geometric average (GA) of the fusing sub-PDFs $f_i(\mathbf{x})$ is given as

$$f_{\text{GA}}(\mathbf{x}) = C^{-1} \prod_{i \in \mathcal{I}} f_i^{w_i}(\mathbf{x}), \quad (15)$$

where $C := \left(\int_{\mathbb{R}^{n_x}} \prod_{i \in \mathcal{I}} f_i^{w_i}(\tilde{\mathbf{x}}) d\tilde{\mathbf{x}} \right)^{-1}$ is the normalization constant. In the linear Gaussian case with respect to estimate pairs $(\hat{\mathbf{x}}_i, \mathbf{P}_i)$, $i \in \mathcal{I}$, the GA-fused result is given as follows

$$\hat{\mathbf{x}}_{\text{GA}}(\mathbf{w}) = \mathbf{P}_{\text{GA}} \sum_{i \in \mathcal{I}} w_i \mathbf{P}_i^{-1} \hat{\mathbf{x}}_i, \quad (16)$$

$$\mathbf{P}_{\text{GA}}(\mathbf{w}) = \left(\sum_{i \in \mathcal{I}} w_i \mathbf{P}_i^{-1} \right)^{-1}. \quad (17)$$

As a special case of the GA fusion, the covariance intersection (CI) fusion optimizes the fusing weights as follows

$$\mathbf{w}_{\text{CI}} = \arg \min_{\mathbf{w} \in \mathbb{W}} \text{Tr}(\mathbf{P}_{\text{GA}}). \quad (18)$$

where $\mathbb{W} := \{\mathbf{w} \in \mathbb{R}^I | \mathbf{w}^T \mathbf{1}_I = 1, w_i > 0, \forall i \in \mathcal{I}\} \subset \mathbb{R}^I$.

That is, $\hat{\mathbf{x}}_{\text{CI}} = \hat{\mathbf{x}}_{\text{GA}}(\mathbf{w}_{\text{CI}})$, $\mathbf{P}_{\text{CI}} = \mathbf{P}_{\text{GA}}(\mathbf{w}_{\text{CI}})$. In this line of research, a variety of approaches have been proposed for further reducing the error covariance metric, leading to various CI-like, less conservative fusion approaches such as the so-called split-CI [42] / bounded covariance inflation [43], ellipsoidal intersection [44], inverse CI (ICI) [45].

In contrary to this trend, it is our observation that the GA fusion is often not too conservative but insufficient in cluttered scenarios which may suffer from out-of-sequential measurement [38] or spurious data [39] and model mismatch. The reason is simply that the fused covariance \mathbf{P}_{CI} as in (17) does not take into account $\hat{\mathbf{x}}_{\text{CI}}$ or any fusing state estimate $\hat{\mathbf{x}}_i$ as both AA and CU fusion have $(\hat{\mathbf{x}}_{AA} - \hat{\mathbf{x}}_i)(\cdot)^T$. If any fusing estimator is covariance inconsistent, the GA fusion will very likely be inconsistent. Then, a more conservative fusion approach like the AA and CU fusion becomes useful. Noticing this, a conservative fusion approach referred to FFCC (fast and fault-tolerant convex combination) that uses smaller fusing weights, namely, $\mathbf{w}^T \mathbf{1}_I = \delta$, where $\delta \leq 1$, was presented in [46]. So, obviously, $\mathbf{P}_{\text{FFCC}} \in [\mathbf{P}_{\text{CI}}, \infty)$.

Summarizing the above results leads to another *conservative fusion chain*:

$$\mathbf{P}_{\text{Naive}} \prec \mathbf{P}_{\text{ICI}} \prec \mathbf{P}_{\text{CI}} \preceq \mathbf{P}_{AA}, \mathbf{P}_{\text{FFCC}}, \quad (19)$$

where $\mathbf{P}_{\text{diff}} = \mathbf{P}_{\text{CI}} = \mathbf{P}_{AA}$ holds iif all fusing estimators are identical, and $\mathbf{P}_{\text{CI}} = \mathbf{P}_{\text{FFCC}}$ holds iif $\delta = 1$.

D. MSE of AA f -Fusion

When the EAP estimator is implemented, the AA f -fusion (6) will lead to the AA v -fusion (5), i.e.,

$$\begin{aligned} \hat{\mathbf{x}}_{AA}^{\text{EAP}} &= \int_{\mathbb{R}^{n_x}} \tilde{\mathbf{x}} f_{AA}(\tilde{\mathbf{x}}) d\tilde{\mathbf{x}} \\ &= \sum_{i \in \mathcal{I}} w_i \int_{\mathbb{R}^{n_x}} \tilde{\mathbf{x}} f_i(\tilde{\mathbf{x}}) d\tilde{\mathbf{x}} \\ &= \sum_{i \in \mathcal{I}} w_i \hat{\mathbf{x}}_i^{\text{EAP}}. \end{aligned} \quad (20)$$

Now, consider the conditionally independent observation process of the true state \mathbf{x} made by sensor $i \in \mathcal{I}$ which generates observations \mathbf{y}_i^n in trial n leading to posteriors $f_i(\mathbf{x}|\mathbf{y}_i^n)$, $n = 1, 2, \dots, N$. Let us define

$$\mathbb{E}_{\mathbf{y}}[\hat{\mathbf{x}}_i] := \frac{1}{N} \sum_{n=1}^N \int_{\mathbb{R}^{n_x}} \tilde{\mathbf{x}} f_i(\tilde{\mathbf{x}}|\mathbf{y}_i^n) d\tilde{\mathbf{x}},$$

$$\Sigma_{\mathbf{y}}(\hat{\mathbf{x}}_i, \hat{\mathbf{x}}_j) := \frac{1}{N-1} \sum_{n=1}^N (\hat{\mathbf{x}}_i|\mathbf{y}_i^n - \mathbb{E}_{\mathbf{y}}[\hat{\mathbf{x}}_i])(\hat{\mathbf{x}}_j|\mathbf{y}_j^n - \mathbb{E}_{\mathbf{y}}[\hat{\mathbf{x}}_j])^T.$$

Then, the conditional unbiasedness and independence of the fusing estimators imply

$$\mathbb{E}_{\mathbf{y}}[\hat{\mathbf{x}}_i] = \mathbf{x}, \forall i \in \mathcal{I}, \quad (21)$$

$$\Sigma_{\mathbf{y}}(\hat{\mathbf{x}}_i, \hat{\mathbf{x}}_j) = \mathbf{0}, \forall i \neq j. \quad (22)$$

Lemma 4. *For a set of unbiased estimators that are conditionally independent to each other as shown in (21) and (22), the AA fusion (20) gains better accuracy in the sense that*

$$\sum_{i \in \mathcal{I}} w_i (\text{MSE}_{\hat{\mathbf{x}}_i} - \text{MSE}_{\hat{\mathbf{x}}_{AA}}) \succ \mathbf{0}. \quad (23)$$

Proof. The proof is straightforward as follows

$$\begin{aligned} \text{MSE}_{\hat{\mathbf{x}}_{AA}} &= \mathbb{E} \left[\left(\mathbf{x} - \sum_{i \in \mathcal{I}} w_i \hat{\mathbf{x}}_i \right) \left(\cdot \right)^T \right] \\ &= \sum_{i \in \mathcal{I}} w_i^2 \text{MSE}_{\hat{\mathbf{x}}_i} + \sum_{i < j \in \mathcal{I}} 2w_i w_j \Sigma_{\mathbf{y}}(\hat{\mathbf{x}}_i, \hat{\mathbf{x}}_j) \end{aligned} \quad (24)$$

$$= \sum_{i \in \mathcal{I}} w_i^2 \text{MSE}_{\hat{\mathbf{x}}_i} \quad (25)$$

$$\prec \sum_{i \in \mathcal{I}} w_i \text{MSE}_{\hat{\mathbf{x}}_i}, \quad (26)$$

where (21) and (22) are used in (24) and (25), respectively. Eq. (26) is due to $w_i > 0, \forall i \in \mathcal{I}, \sum_{i \in \mathcal{I}} w_i = 1$. \square

When $\text{MSE}_{\hat{\mathbf{x}}_i} = \text{MSE}_{\hat{\mathbf{x}}_j}, w_i = w_j, \forall i \neq j \in \mathcal{I}$, (25) will reduce to $\text{MSE}_{\hat{\mathbf{x}}_{AA}} = \frac{1}{|\mathcal{I}|} \text{MSE}_{\hat{\mathbf{x}}_i}$, which indicates that the AA fusion can significantly benefit in gaining lower MSE in the case that all fusing estimators have equivalent MSEs and are conditionally independent of each other. This does not matter what are their respective associated error covariances. In fact, if these fusing estimators are overall negatively correlated, e.g., $\sum_{i < j \in \mathcal{I}} 2w_i w_j \Sigma_{\mathbf{y}}(\hat{\mathbf{x}}_i, \hat{\mathbf{x}}_j) \prec \mathbf{0}$, the AA fusion gain will be more significant than what stated in (23).

E. Empirical Study: Mode-preservation in AA Fusion

There is a prevailing oversimplification of the relationship between the variance and the accuracy of the fused estimate since the influential work [47]. As indicated in Definition 1, they are not the same: a smaller variance associated with the fused estimate does not directly imply a better estimate whether in the sense of MMSE or Bayes optimality. In fact, the setting of a reasonably large noise variance (which will result in a large filter estimate covariance) can accommodate model mismatches [48], [49] and in dealing with the degeneracy of the particle filter [50].

To gain insight from a simple example—which is consistent with the example used in [47]—two Gaussian probability densities with different means and covariances are considered. Four representative scenarios are illustrated in (a), (b), (c) and (d) of Fig. 1, respectively, where the two Gaussian densities to be fused are visualized by two ellipses P1 and P2 that characterize the respective covariances, with the center points indicating the respective means. We consider the aforementioned fusion schemes: the naive fusion (14), un-weighted GA fusion (i.e., (16) and (17) using $w_1 = w_2 = 0.5$), CI fusion (i.e., (16) and (17) using optimized weight as (18) which results in $w_1 = 0.3764, w_2 = 0.6236$ in this case), un-weighted AA fusion (i.e., (5) and (10) using $w_1 = w_2 = 0.5$) with and without component merging, and two versions of the CU fusion with fused covariance given as in (8) (referred to as CU max) and in (9) (referred to as CU min), respectively. These results verify the two conservative fusion chains (13) and (19): First, all these conservation fusion approaches lead to obvious covariance inflation as compared with the naive fusion. Second, the CU and AA fusion has more or less greater inflation than the GA/CI fusion.

In all four scenarios, without the knowledge of the true target position, we cannot tell whether any of the seven fusion schemes is better than the others, no matter their estimate is given by the EAP or MAP. Even in scenario (a) there is no guarantee that the target is localized in the intersection of P1 and P2; if it is not, then both naive fusion and GA/CI fusion will likely produce incorrect results. In scenarios (c) and (d), at least one of P1 and P2 is inconsistent whatever it may be⁴. In these cases, the AA fusion may not merge two densities to one but keep a multimodal FMD to avoid producing inconsistent or incorrect results; in time-series, new data will help identify the false/inconsistent components and prune them if any. This makes the AA fusion which preserves the modes of the FMD compelling for time-series estimation fusion. In practice, the MAP estimator is usually implemented in a simplified way which extracts the greatest weighted MAP/mode of the fusing estimators as in (27) (or multiple in the case of multi-target estimation), rather than calculating the real mode of the fused density as a whole as in (28).

$$\hat{\mathbf{x}}_{AA}^{\text{MAP}} := \hat{\mathbf{x}}_{j=\arg \max_{i \in \mathcal{I}} w_i}^{\text{MAP}}, \quad (27)$$

$$\hat{\mathbf{x}}_{AA}^{\text{MAP}} = \arg \sup_{\tilde{\mathbf{x}} \in \mathbb{R}^{n_x}} f_{AA}(\tilde{\mathbf{x}}). \quad (28)$$

The common choice (27) leads to a mode-preservation capacity which reinforces the tolerance of the AA fusion to inconsistent fusing estimators or even fault estimators, namely “*fault-tolerant*”, leading to an unique feature of the AA fusion: When the fusing distributions diverge significantly with each other such as in (d), it will not merge them into one but only re-weight them and preserve the original modes; so is done in existing AA fusion approaches where merging is only carried out to the components close enough to each other and MAP is often approximately applied as shown in (27) [8]–[16].

⁴This is common in mixture-type filters, since at any specific time-instant, the centers of most components do not necessarily conform to the state of any target—due to the randomness of the state and of the observation—even through the mixture filter as a whole is statistically unbiased.

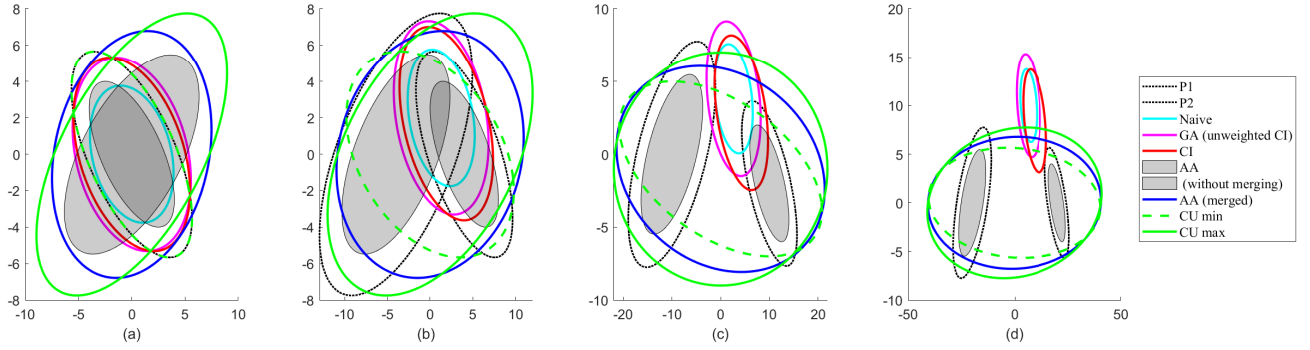


Fig. 1. Fusing two Gaussian densities having four different levels of divergences, using naive fusion, GA fusion, AA fusion or CU fusion, all using the same fusing weights. (a): two densities overlap largely and both estimators are likely to be conservative. (b): two densities are offset from each other but still overlap somehow. (c) and (d): two densities are greatly offset from each other and at most one estimator is conservative. Note: when the fusing weights are optimized as in (18), the GA fusion reduces to the CI fusion. The naive AA fusion is given by the combination of the two densities which are re-weighted forming a multimodal FMD but may not be merged to one in practice. Merging should only be applied when mixands are close significantly to each other. What has been shown in blue is the merged result, which is only reasonable when the mixands are close, like in (a), but not in (d).

There is a theoretical explanation. Recall that the AA and GA fusion rules symmetrically minimize the weighted sum of the directional KL divergences between the fusing probability distributions and the fused result as follows [51], [52]

$$f_{AA}(\mathbf{x}) = \arg \min_{g: \mathbb{R}^{n_x} \rightarrow \mathbb{R}} \sum_{i \in \mathcal{I}} w_i D_{KL}(f_i \| g), \quad (29)$$

$$f_{GA}(\mathbf{x}) = \arg \min_{g: \int_{\mathbb{R}^{n_x}} g(\mathbf{x}) d\mathbf{x} = 1} \sum_{i \in \mathcal{I}} w_i D_{KL}(g \| f_i). \quad (30)$$

It has been pointed out in [53] that the forward KL divergence as shown in (30) but not (29) has a tendency towards the merging operation no matter how separated the mixands are; see illustrative examples studied therein. Such a tendency may be preferable in applications such as MMSE/EAP based estimation, but may lead to a loss of the important details of the mixture, e.g., the mode, which is less desirable in MAP-based estimation and in multi-target estimation.

III. INFORMATION DIVERGENCE IN BAYESIAN VIEWPOINT

In the Bayesian formulation, the real state is considered random and the posterior is given in the manner of an estimate $f(\mathbf{x})$ to the true distribution $p(\mathbf{x})$ of \mathbf{x} (or $p(\mathbf{X})$ of a multi-target set \mathbf{X}). Without loss of generality, we still consider the single-target density fusion. In this section we use the KL divergence to measure the quality of distribution $f(\mathbf{x})$ with regard to the real state distribution $p(\mathbf{x})$.

A. Mixture Fit

Lemma 5. For a number of probability distributions $f_i(\mathbf{x})$, $i \in \mathcal{I}$, the KL divergence of the target distribution $p(\mathbf{x})$ relative to their average $f_{AA}(\mathbf{x})$ is given as

$$D_{KL}(f_{AA} \| p) = \sum_{i \in \mathcal{I}} w_i (D_{KL}(f_i \| p) - D_{KL}(f_i \| f_{AA})), \quad (31)$$

$$\leq \sum_{i \in \mathcal{I}} w_i D_{KL}(f_i \| p), \quad (32)$$

where the last equation holds iff all fusing sub-distributions $f_i(\mathbf{x})$, $i \in \mathcal{I}$ are identical.

Proof. The proof is straightforward as follows

$$\begin{aligned} D_{KL}(f_{AA} \| p) &= \int_{\mathbb{R}^{n_x}} \sum_{i \in \mathcal{I}} w_i f_i(\mathbf{x}) \log \frac{f_{AA}(\mathbf{x})}{g(\mathbf{x})} \delta \mathbf{x} \\ &= \sum_{i \in \mathcal{I}} w_i \left(\int_{\mathbb{R}^{n_x}} f_i(\mathbf{x}) \log \frac{f_i(\mathbf{x})}{g(\mathbf{x})} \delta \mathbf{x} \right. \\ &\quad \left. - \int_{\mathbb{R}^{n_x}} f_i(\mathbf{x}) \log \frac{f_i(\mathbf{x})}{f_{AA}(\mathbf{x})} \delta \mathbf{x} \right) \\ &= \sum_{i \in \mathcal{I}} w_i (D_{KL}(f_i \| p) - D_{KL}(f_i \| f_{AA})) \\ &\leq \sum_{i \in \mathcal{I}} w_i D_{KL}(f_i \| p), \end{aligned}$$

where the equation holds iff $D_{KL}(f_i \| f_{AA}) = 0$, $\forall i \in \mathcal{I}$, namely, all sub-distributions f_i , $i \in \mathcal{I}$ are identical. \square

Similar results have been given earlier in the textbook [54, Theorem 4.3.2]. Noticing that the KL divergence function is convex, (32) can also be proved by using Jensen's inequality [55, Ch. 2.6]. This result indicates that the average of the mixture fits the target distribution better than all mixands on average. We will show next that optimized mixing weights will accentuate the benefit of fusion.

B. Fusing Weight

The naive weighting solution is the normalized uniform weights, namely $\mathbf{w} = \mathbf{1}_I / S$. That is, all fusing estimators are treated equally which makes sense for fusing information from homogeneous sources. This is simple but does not distinguish online the information of high quality from that of low at any particular time. More convincingly, the optimal solution should minimize $D_{KL}(f_{AA} \| p)$ in order to best fit the target distribution, i.e.,

$$\mathbf{w}_{\text{opt}} = \arg \min_{\mathbf{w} \in \mathbb{W}} \sum_{i \in \mathcal{I}} w_i (D_{KL}(f_i \| p) - D_{KL}(f_i \| f_{AA})). \quad (33)$$

As shown above, the component that fits the target distribution better (corresponding to smaller $D_{KL}(f_i \| p)$) and greater

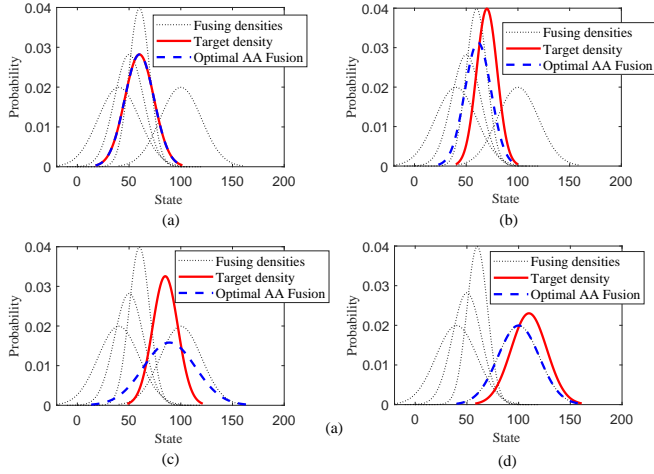


Fig. 2. Optimal AA fusion of four Gaussian densities (each given by a black dotted line) to best fit the target density (red solid line) in four different cases, resulting in the optimally merged Gaussian density (blue dashed line).

$D_{\text{KL}}(f_i \| f_{\text{AA}})$ deserves a greater fusing weight. However, the target distribution $p(\mathbf{x})$ is typically unknown or too complicated to be practically useful, so is $D_{\text{KL}}(f_i \| p)$. It is also obvious that even if the true distribution $p(\mathbf{x})$ is available, the knowledge $D_{\text{KL}}(f_i \| p) < D_{\text{KL}}(f_j \| p)$, $\forall j \neq i$ does not necessarily result in $w_i = 1, w_j = 0, \forall j \neq i$. It depends on $D_{\text{KL}}(f_i \| f_j)$, $\forall j \neq i$. In other words, when the fusing weights are properly designed, the arithmetically averaged mixture may fit the target distribution better than the best component. This can be easily illustrated by examples as given in Fig. 2. The four densities to be fused are $f_1(\mathbf{x}) = \mathcal{N}(\mathbf{x}; 40, 400)$, $f_2(\mathbf{x}) = \mathcal{N}(\mathbf{x}; 50, 200)$, $f_3(\mathbf{x}) = \mathcal{N}(\mathbf{x}; 60, 100)$, $f_4(\mathbf{x}) = \mathcal{N}(\mathbf{x}; 100, 400)$, respectively. For four different target densities such as $p(\mathbf{x}) = \mathcal{N}(\mathbf{x}; 60, 200)$, $\mathcal{N}(\mathbf{x}; 70, 100)$, $\mathcal{N}(\mathbf{x}; 85, 150)$, and $\mathcal{N}(\mathbf{x}; 110, 300)$, the optimal merging weights according to (39) are given by $\mathbf{w}_{\text{opt}} = [0.0256, 0.0855, 0.8547, 0.0342]^T$, $[0, 0, 0.966, 0.034]^T$, $[0, 0, 0.2738, 0.7262]^T$ and $[0, 0, 0, 1]^T$ resulting in the AA density $f_{\text{AA}}(\mathbf{x}) = \mathcal{N}(\mathbf{x}; 60, 200)$, $\mathcal{N}(\mathbf{x}; 61.36, 162.82)$, $\mathcal{N}(\mathbf{x}; 89.05, 635.98)$, $\mathcal{N}(\mathbf{x}; 100, 400)$, respectively. Only in the last case where the means of all fusing densities coincidentally lie on the same side of that of the target density, the optimal result is given by the single best density.

A simplified, practically operable, alternative is ignoring the former part in (33) which will then reduce to the following suboptimal maximization problem

$$\mathbf{w}_{\text{subopt}} = \arg \max_{\mathbf{w} \in \mathbb{W}} \sum_{i \in \mathcal{I}} w_i D_{\text{KL}}(f_i \| f_{\text{AA}}) \quad (34)$$

$$= \arg \max_{\mathbf{w} \in \mathbb{W}} \sum_{i \in \mathcal{I}} w_i (H(f_i, f_{\text{AA}}) - H(f_i)). \quad (35)$$

where $H(f, g) := -\int_{\mathbb{R}^{n_x}} f(\mathbf{x}) \log g(\mathbf{x}) \delta \mathbf{x}$ is the cross-entropy of distributions f and g , also called Shannon entropy, and $H(f) := H(f, f)$ is the differential entropy of $f(\mathbf{x})$.

The suboptimal, practically operable, optimization given by (34) assigns a greater fusing weight to the distribution that diverges more from the others. This can be referred to as a *diversity preference* solution. Alternatively, one may resort

to some functionally-similar divergences or metrics to assign higher weights to the components that fit the data better, namely *likelihood preference*.

Nevertheless, the fusing weights can be determined for some other purposes, e.g., in the context of seeking consensus over a peer-to-peer network, they are often designed for ensuring fast convergence [8]–[10], [15], [16].

C. Max-Min Optimization

Recall the divergence minimization (29) that the AA fusion admits [10], [52]. Now, combining (29) with (34) yields joint optimization of the fusing form and fusing weights as follows

$$f_{\text{AA}}(\mathbf{w}_{\text{subopt}}) = \arg \max_{g(\mathbf{w})} \min_{\mathbf{w} \in \mathbb{W}} \sum_{i \in \mathcal{I}} w_i D_{\text{KL}}(f_i \| g). \quad (36)$$

This variational fusion problem (36) resembles that for geometric average (GA) fusion [56], [57], i.e., $f_{\text{GA}}(\mathbf{w}_{\text{subopt}}) = \arg \max_{g(\mathbf{w})} \min_{\mathbf{w} \in \mathbb{W}} \sum_{i \in \mathcal{I}} w_i D_{\text{KL}}(g \| f_i)$. It has actually been pointed out that the suboptimal fusion results for both variational fusion problems have equal KL divergence from/to the fusing sub-distributions [56]. That is, $\forall i \neq j \in \mathcal{I}$,

$$D_{\text{KL}}(f_i \| f_{\text{AA}}(\mathbf{w}_{\text{subopt}})) = D_{\text{KL}}(f_j \| f_{\text{AA}}(\mathbf{w}_{\text{subopt}})), \quad (37)$$

$$D_{\text{KL}}(f_{\text{GA}}(\mathbf{w}_{\text{subopt}}) \| f_i) = D_{\text{KL}}(f_{\text{GA}}(\mathbf{w}_{\text{subopt}}) \| f_j), \quad (38)$$

which implies that the suboptimal, diversity preference fusion tends to revise all fusing estimators equivalently, resulting in a middle distribution where the AA and GA differs from each other due to the asymmetry of the KL divergence.

Derivation for (38) has been earlier given in [33], [58] which is related to the Chernoff information [55], [59]. Weighted middle is suggested in [60] which assigns different weights on both sides of (38).

D. Case Study: Gaussian Fusion

We now consider the special case of Gaussian PDF. The KL divergence of $f_1(\mathbf{x}) := \mathcal{N}(\mathbf{x}; \mu_1, \mathbf{P}_1)$ relative to $f_2(\mathbf{x}) := \mathcal{N}(\mathbf{x}; \mu_2, \mathbf{P}_2)$ is given as

$$D_{\text{KL}}(\mathcal{N}(\mu_1, \mathbf{P}_1) \| \mathcal{N}(\mu_2, \mathbf{P}_2)) = \frac{1}{2} \left[\text{tr}(\mathbf{P}_2^{-1} \mathbf{P}_1) - n_x + \log \frac{\det(\mathbf{P}_2)}{\det(\mathbf{P}_1)} + \|\mu_1 - \mu_2\|_{\mathbf{P}_2}^2 \right],$$

where $\|\mu_1 - \mu_2\|_{\mathbf{P}}^2 := (\mu_1 - \mu_2)^T \mathbf{P}^{-1} (\mu_1 - \mu_2)$.

Unfortunately, there is no such analytical expression for the KL divergence between two GMs or even between a Gaussian and a GM. A number of approximate, exactly-expressed approaches have been investigated [61]. In the following we consider two alternatives.

1) *Moment Matching-Based Approximation*: The first is merging the mixture to a single Gaussian PDF, or to say, fitting the GM PDF by a single Gaussian PDF. Then, the divergence of two GMs or between a Gaussian PDF and a GM can be approximated by that between their best-fitting Gaussian PDFs. As given in Lemma 3, the moment fitting Gaussian PDF for a GM $f_i(\mathbf{x}) = \mathcal{N}(\mathbf{x}; \mu_i, \mathbf{P}_i)$, $i \in \mathcal{I}$ is $f_{\text{AA,merged}}(\mathbf{x}) = \mathcal{N}(\mathbf{x}; \mu_{\text{AA}}, \mathbf{P}_{\text{AA}})$, where $\mu_{\text{AA}} = \sum_{i \in \mathcal{I}} w_i \mu_i$, $\mathbf{P}_{\text{AA}} = \sum_{i \in \mathcal{I}} w_i (\mathbf{P}_i + (\mu_{\text{AA}} - \mu_i)(\cdot)^T)$. Using

$f_{AA,merged}(\mathbf{x})$ for approximately fitting the target Gaussian PDF $p(\mathbf{x}) = \mathcal{N}(\mathbf{x}; \mu, \mathbf{P})$ yields

$$\begin{aligned} \mathbf{w}_{opt} &\approx \arg \min_{\mathbf{w} \in \mathbb{W}} D_{KL}(\mathcal{N}(\mu_{AA}, \mathbf{P}_{AA}) \parallel \mathcal{N}(\mu, \mathbf{P})) \\ &= \arg \min_{\mathbf{w} \in \mathbb{W}} \left[\text{tr}(\mathbf{P}^{-1} \mathbf{P}_{AA}) + \log \frac{\det(\mathbf{P})}{\det(\mathbf{P}_{AA})} \right. \\ &\quad \left. + \|\mu_{AA} - \mu\|_{\mathbf{P}}^2 \right]. \end{aligned} \quad (39)$$

When the target distribution is unknown and the diversity preference solution as given in (34) is adopted, one has

$$\begin{aligned} \mathbf{w}_{subopt} &\approx \arg \max_{\mathbf{w} \in \mathbb{W}} \sum_{i \in \mathcal{I}} w_i D_{KL}(f_i \parallel f_{AA,merged}) \\ &= \arg \max_{\mathbf{w} \in \mathbb{W}} \sum_{i \in \mathcal{I}} w_i \left[\text{tr}(\mathbf{P}_{AA}^{-1} \mathbf{P}_i) + \log \frac{\det(\mathbf{P}_{AA})}{\det(\mathbf{P}_i)} \right. \\ &\quad \left. + \|\mu_i - \mu_{AA}\|_{\mathbf{P}_{AA}}^2 \right]. \end{aligned} \quad (40)$$

Note that as explained in section II-E and in [53], the merging operation may lead to a loss of the important feature of the mixture, such as the mode. More general result of the KL divergence between multivariate generalized Gaussian distributions can be found in [62]. The KL divergence between two Bernoulli random finite set distributions with Gaussian single target densities is given in [63].

2) *Bound Optimization*: Using Jensen's inequality on the convex function $-\log(\mathbf{x})$, i.e., $f(\mathbb{E}[\mathbf{x}]) \leq \mathbb{E}[f(\mathbf{x})]$, a lower bound can be found for $H(f_i, f_{AA})$ as

$$\begin{aligned} H(f_i, f_{AA}) &= - \int_{\mathbb{R}^{n_x}} f_i(\mathbf{x}) \log f_{AA}(\mathbf{x}) \delta \mathbf{x} \\ &\geq - \log \left(\int_{\mathbb{R}^{n_x}} f_i(\mathbf{x}) f_{AA}(\mathbf{x}) \delta \mathbf{x} \right) \\ &= - \log \left(\sum_{j \in \mathcal{I}} w_j \int_{\mathbb{R}^{n_x}} f_i(\mathbf{x}) f_j(\mathbf{x}) \delta \mathbf{x} \right). \end{aligned} \quad (41)$$

Denote the integration of the product of two Gaussian PDFs $f_i(\mathbf{x}) = \mathcal{N}(\mathbf{x}; \mu_i, \mathbf{P}_i)$ and $f_j(\mathbf{x}) = \mathcal{N}(\mathbf{x}; \mu_j, \mathbf{P}_j)$ as $z_{i,j}$, namely,

$$\int_{\mathbb{R}^{n_x}} f_i(\mathbf{x}) f_j(\mathbf{x}) \delta \mathbf{x} = \mathcal{N}(\mu_i; \mu_j, \mathbf{P}_i + \mathbf{P}_j) := z_{i,j}. \quad (42)$$

Furthermore, for a single Gaussian density $f_i(\mathbf{x}) = \mathcal{N}(\mathbf{x}; \mu_i, \mathbf{P}_i)$, the differential entropy is given by

$$H(f_i) = \frac{1}{2} \log((2\pi e)^{n_x} |\mathbf{P}_i|). \quad (43)$$

Combing (41), (42) and (43) leads to

$$\begin{aligned} D_{KL}(f_i \parallel f_{AA}) &= (H(f_i, f_{AA}) - H(f_i)) \\ &\geq - \log \left((2\pi e)^{\frac{n_x}{2}} |\mathbf{P}_i|^{\frac{1}{2}} \sum_{j \in \mathcal{I}} w_j z_{i,j} \right). \end{aligned} \quad (44)$$

This is useful for solving the suboptimal optimization problem (35) as maximizing the lower bounds implies maximizing the content. That is,

$$\begin{aligned} \mathbf{w}_{subopt} &= \arg \max_{\mathbf{w} \in \mathbb{W}} \sum_{i \in \mathcal{I}} w_i D_{KL}(f_i \parallel f_{AA}) \\ &\approx \arg \min_{\mathbf{w} \in \mathbb{W}} \sum_{i \in \mathcal{I}} w_i \log \left(|\mathbf{P}_i|^{\frac{1}{2}} \sum_{j \in \mathcal{I}} w_j z_{i,j} \right). \end{aligned} \quad (45)$$

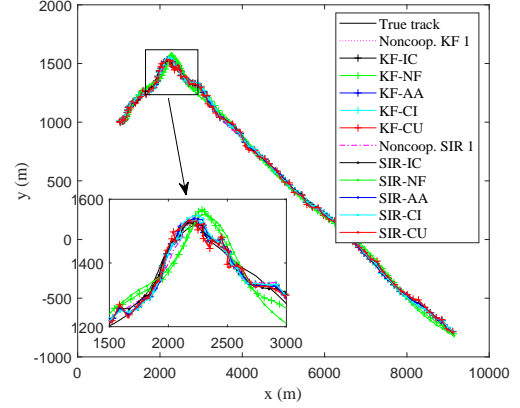


Fig. 3. The ground truth of the target trajectory, the estimates of the noncooperative filters and their two-sensor-fusion results in the linear scenario.

IV. SIMULATIONS

We considered two representative single-target tracking scenarios, based on either linear or nonlinear state space models. In each scenario, the simulation is performed for 100 Monte Carlo runs, each having 100 filtering steps. We note that comprehensive comparison of some of the aforementioned conservative fusion approaches in more complicated sensor-network-based multi-target tracking scenarios in the presence of false and missing data are available in the references, e.g., [8]–[10], [13], [14], [16], [64], [65]. Here, we limit our simulation study to the bare case having no false and missing data and having merely two sensors in order to gain the insight of the performance of these fusion approaches in perfectly modelled scenarios. This does not so match the purpose of fault-tolerant fusion such as the CU approach that is designed particularly for fusion involving inconsistent estimators.

The root mean square error (RMSE) is a suitable metric for accuracy evaluation. The base filters we adopted are the benchmark Kalman filter (KF) / cubature KF (CKF) [66] (for the linear and nonlinear models, respectively) and the sampling importance resampling (SIR) particle filter. It is known that, for the linear Gaussian model, the KF provides the exact, optimal solution. The SIR filter is a Bayesian filter based on Monte Carlo simulation for which we use $N_p = 200, 500$ particles in the linear and nonlinear model, respectively.

Comparison fusion methods are the naive fusion (NF) using (14), the CI fusion using (18), the CU fusion using (8) and the AA fusion using (40). In addition to these density fusion approaches we also consider the noncooperative single-sensor KF/CKF/SIR filters (that use the measurements of Sensor 1 only) and the iterated-corrector (IC) algorithm for fusing the measurements of two sensors. In the IC approach, the measurements of two sensors are used in sequence in the filters, which amounts to calculating the joint likelihood by multiplying their respective likelihoods, i.e.,

$$p(\mathbf{y}_{1,k}, \mathbf{y}_{2,k} | \mathbf{x}_k) = p(\mathbf{y}_{1,k} | \mathbf{x}_k) p(\mathbf{y}_{2,k} | \mathbf{x}_k), \quad (46)$$

where $\mathbf{y}_{1,k}$ and $\mathbf{y}_{2,k}$ are the measurements of the target generated at sensor 1 and 2 at time k , respectively.

Given that the measurements of two sensors are uncorrelated, the IC approach is Bayesian optimal. The posterior densities yielded by the KFs/CKFs are Gaussian PDFs of which the NF, CI, CU fusion all result in a single Gaussian PDF. In contrast, the AA fusion of two Gaussian PDFs is a GM of two components for which we apply the merging scheme [40] to maintain closed-form Gaussian recursion as required in KFs/CKFs. For the SIR filters, the AA fusion of two particle distributions remains a particle distribution (of a larger size namely $2N_p$ if two are merged into one) which is an advantage of the AA fusion. However, in order to apply the NF, CI and CU fusion approach to the SIR filters, it is necessary to convert those particles to a parametric distribution for which we apply the Gaussian PDF. This particles-to-Gaussian conversion is also used in the AA fusion in order to calculate the suboptimal fusion weight (40). After the fusion, N_p new particles are resampled from the fused Gaussian PDF [67].

A. Linear Scenario

In our first simulation, the state of the target $\mathbf{x}_k = [p_{x,k}, \dot{p}_{x,k}, p_{y,k}, \dot{p}_{y,k}]^T$ consists of planar position $[p_{x,k}, p_{y,k}]^T$ and velocity $[\dot{p}_{x,k}, \dot{p}_{y,k}]^T$. At time $k = 0$, it is randomly initialized as $\mathbf{x}_0 \sim \mathcal{N}(\mathbf{x}; \mu_0, \mathbf{P}_0)$, where $\mu_0 = [1000\text{m}, 20\text{m/s}, 1000\text{m}, 0\text{m/s}]^T$ with $\mathbf{Q} =$ and $\mathbf{P}_0 = \text{diag}\{[500\text{m}^2, 50\text{m}^2/\text{s}^2, 500\text{m}^2, 50\text{m}^2/\text{s}^2]\}$, where $\text{diag}\{\mathbf{a}\}$ represents a diagonal matrix with diagonal \mathbf{a} . The target moves following a nearly constant velocity motion given as (with the sampling interval $\Delta = 1\text{s}$)

$$\mathbf{x}_k = \begin{bmatrix} 1 & \Delta & 0 & 0 \\ 0 & 1 & 0 & 0 \\ 0 & 0 & 1 & \Delta \\ 0 & 0 & 0 & 1 \end{bmatrix} \mathbf{x}_{k-1} + \begin{bmatrix} \frac{\Delta^2}{2} & 0 \\ \Delta & 0 \\ 0 & \frac{\Delta^2}{2} \\ 0 & \Delta \end{bmatrix} \mathbf{u}_{k-1}, \quad (47)$$

where the process noise $\mathbf{u}_k \sim \mathcal{N}(\mathbf{u}; \mathbf{0}_2\text{m/s}^2, 25\mathbf{I}_2\text{m}^2/\text{s}^4)$.

Both sensors have the following linear measurement model

$$\mathbf{y}_k = \begin{bmatrix} 1 & 0 & 0 & 0 \\ 0 & 0 & 1 & 0 \end{bmatrix} \mathbf{x}_k + \begin{bmatrix} v_{k,1} \\ v_{k,2} \end{bmatrix}, \quad (48)$$

with $v_{k,1}$ and $v_{k,2}$ as mutually independent zero-mean Gaussian noise with the same standard deviation R . For sensor 1, it is $R = 20\text{m}$ while for sensor 2, it is $R = 40\text{m}$. That is to say, sensor 1 has a better quality than sensor 2.

The real trajectory of the target and the estimates of the noncooperative and of two-sensor-fusion KF and SIR filters in one trial are given in Fig. 3. The RMSEs of these filters are given in Fig. 4 and Fig. 5 in terms of the position and velocity estimation, respectively. The average RMSEs over all filtering times are given in Table I. As shown, the average performance of the NF based filters namely KF-NF and SIR-NF is the worst in all, even much worse than the noncooperative filters that apply no fusion. The CU-based filters are the second worst. This is probably because the former completely omits the cross-correlation between two sensors leading to inconsistent fused result, while the latter is over conservative leading to inaccurate results. As expected, the exactly Bayes-optimal KF-IC filter performs the best in all. The AA fusion performs similar with the CI fusion in both cases of KF and SIR filters,

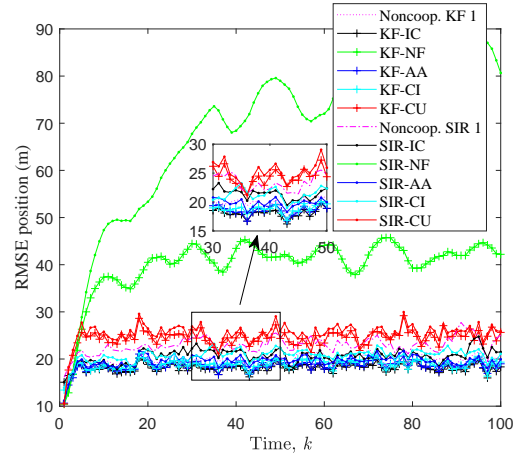


Fig. 4. The position RMSEs of noncooperative and two-sensor-fusion filters in the linear scenario.

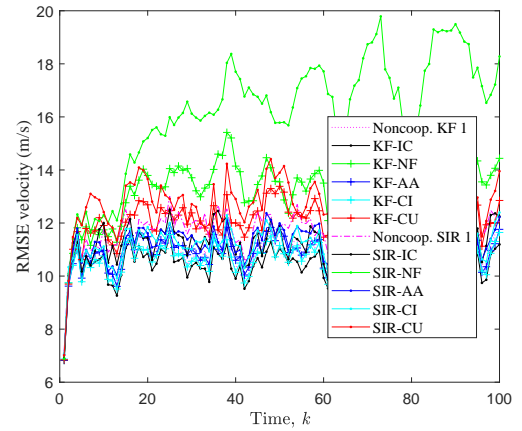


Fig. 5. The velocity RMSEs of noncooperative and two-sensor-fusion filters in the linear scenario.

close to the best IC filters. These comparison results imply that the AA and CI fusion obtain a good balance between conservative and informative. When any of NF, AA, CI, CU or IC is applied for fusion or in the noncooperative mode, the KF slightly outperforms the SIR filter in this linear Gaussian scenario as expected.

Further on, the average and variance of the fusion weight assigned to sensor 1 in the KF-AA fusion are given in Fig. 6. The results show that, the average fusion weight assigned to sensor 1 is about 0.575 with a small variance, which indicates that the weighting solution (40) indeed makes sense as it assigns a greater weight to the sensor of better quality.

B. Nonlinear Scenario

In the second scenario, the target state is denoted as $\mathbf{x}_k = [p_{x,k}, \dot{p}_{x,k}, p_{y,k}, \dot{p}_{y,k}, \omega_k]^T$ with an additional turn rate ω_k as compared with that in the last simulation. It is randomly initialized as follows $\mathbf{x}_0 \sim \mathcal{N}(\mathbf{x}; \mu_0, \mathbf{P}_0)$, where $\mu_0 = [1000\text{m}, 20\text{m/s}, 1000\text{m}, 0\text{m/s}, -\pi/60\text{rad}]^T$ with $\mathbf{Q} =$ and $\mathbf{P}_0 = \text{diag}\{[500\text{m}^2, 50\text{m}^2/\text{s}^2, 500\text{m}^2, 50\text{m}^2/\text{s}^2, 0.01\text{rad}^2]\}$. The target moves following a coordinated turn model with

TABLE I
AVERAGE RMSE OF DIFFERENT FILTERS IN THE LINEAR SCENARIO.

Filter	ARMSE position [m]	ARMSE velocity [m/s]
Noncoop. KF 1	19.95	10.86
KF-IC	18.13	10.51
KF-NF	39.99	13.32
KF-AA	18.57	10.91
KF-CI	18.85	10.70
KF-CU	24.36	12.06
Noncoop. SIR 1	22.90	11.74
SIR-IC	20.62	11.36
SIR-NF	66.07	16.16
SIR-AA	19.55	11.30
SIR-CI	20.76	11.23
SIR-CU	25.42	12.72

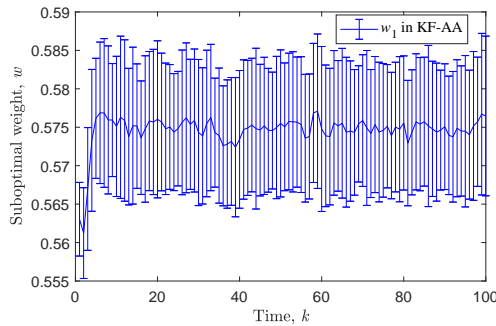


Fig. 6. The average and variance of the fusion weight assigned to sensor 1 in the KF-AA fusion in the linear scenario.

a sampling period of $\Delta = 1$ s and transition density $f_{k|k-1}(\mathbf{x}_k|\mathbf{x}_{k-1}) = \mathcal{N}(\mathbf{x}_k; F(\omega_k)\mathbf{x}_{k-1}, \mathbf{Q})$, where

$$F(\omega) = \begin{bmatrix} 1 & \frac{\sin \omega \Delta}{\omega} & 0 & \frac{1 - \cos \omega \Delta}{\omega} & 0 \\ 0 & \cos \omega \Delta & 0 & -\sin \omega \Delta & 0 \\ 0 & \frac{1 - \cos \omega \Delta}{\omega} & 1 & \frac{\sin \omega \Delta}{\omega} & 0 \\ 0 & \sin \omega \Delta & 0 & \cos \omega \Delta & 0 \\ 0 & 0 & 0 & 0 & 1 \end{bmatrix}, \quad (49)$$

and $\mathbf{Q} = \text{diag}([\mathbf{I}_2 \otimes \mathbf{G}, \sigma_u^2])$ with $\mathbf{G} = q_1 \begin{bmatrix} \frac{\Delta^3}{3} & \frac{\Delta^2}{2} \\ \frac{\Delta^2}{2} & \Delta \end{bmatrix}$, where \otimes is the Kronecker product, $q_1 = 0.1$, and $\sigma_u^2 = 10^{-4}$ rad/s.

Sensor $s \in \{1, 2\}$ localized at $[x_s; y_s]$ generates the range-bearing measurement as

$$\mathbf{y}_{s,k} = \begin{bmatrix} \sqrt{(p_{x,k} - x_s)^2 + (p_{y,k} - y_s)^2} \\ \tan^{-1}\left(\frac{p_{y,k} - y_s}{p_{x,k} - x_s}\right) \end{bmatrix} + \begin{bmatrix} r_{s,k} \\ \theta_{s,k} \end{bmatrix}, \quad (50)$$

where $r_{s,k}$ and $\theta_{i,k}$ are zero-mean Gaussian with standard deviation σ_r m and σ_θ rad, respectively. They are $x_1 = 0$ m, $y_1 = 0$ m, $\sigma_r = 10$ m and $\sigma_\theta = -\pi/180$ rad for sensor 1 and $x_2 = 500$ m, $y_2 = 0$ m, $\sigma_r = 20$ m and $\sigma_\theta = -\pi/90$ rad for sensor 2, respectively.

The trajectory of the target, as well as the estimates of the noncooperative and two-sensor-fusion CKF and SIR filters, in one trial is given in Fig. 7. The RMSEs of these noncooperative and two-sensor-fusion filters are given in Fig. 8, Fig.

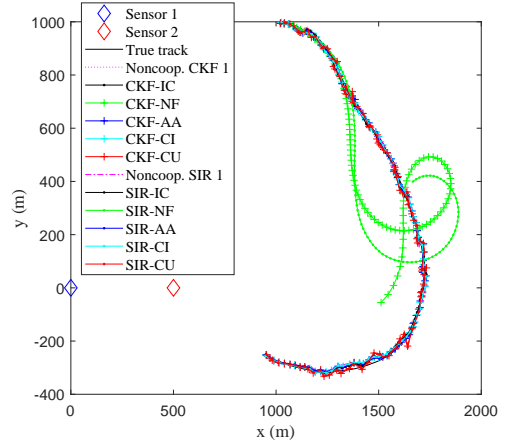


Fig. 7. The position of the two sensors, the ground truth of the target trajectory, the estimates of the noncooperative filters and their two-sensor-fusion results in the nonlinear scenario.

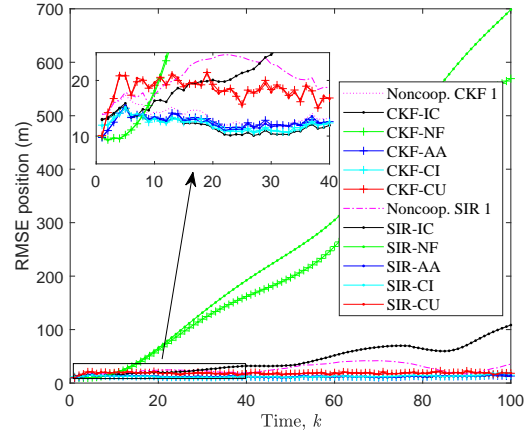


Fig. 8. The position RMSEs of noncooperative and two-sensor-fusion filters in the nonlinear scenario.

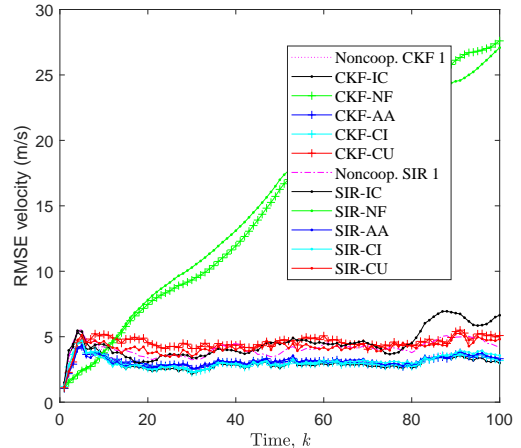


Fig. 9. The velocity RMSEs of noncooperative and two-sensor-fusion filters in the nonlinear scenario.

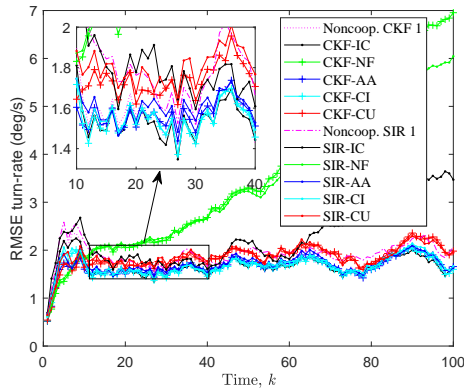


Fig. 10. The turn-rate RMSEs of noncooperative and two-sensor-fusion filters in the nonlinear scenario.

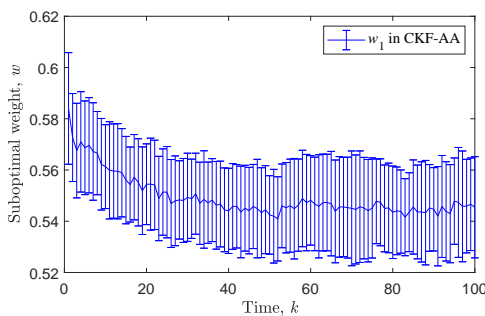


Fig. 11. The average and variance of the fusion weight assigned to sensor 1 in the CKF-AA fusion in the nonlinear scenario.

9 and Fig. 10 in terms of the position, velocity and turn-rate estimation, respectively. The average RMSEs over all filtering times are given in Table II. These results are consistent with those in the linear scenarios. As shown in Fig. 7, the estimates of CKF/SIR-NF filters corrupt as they diverge significantly from the true trajectory, leading an average performance that is to a large degree worse than the others. The failure of the NF in this scenario just exposes the risk of inconsistent/over-positive fusion. Again, the CU-based filters under-perform the NF filters, due to its over-conservativeness. As a trade-off between conservative and informative, the AA and CI fusion-based filters perform the best in whether CKF or SIR filters, close to the IC-CKF filters. Differing from what shown in the last simulation, the SIR filters perform slightly better than the CKF filters except the SIR-IC which performs much worse than the CKF-IC filter and even the SIR-CU filters. This is possibly because the joint likelihood (46) is very informative which can easily cause particle degeneracy [67] and so deteriorate the filter. Both AA and CI fusion are free of this problem. The average and variance of the fusion weight assigned to sensor 1 in the CKF-AA fusion are given in Fig. 11. It shows that the average fusing weight assigned to sensor 1 gradually reduces from 0.584 to 0.541, implying that sensor 1 has been reasonably assigned with a greater fusion weight. The slight reduction of the fusing weight may due to that both filters perform closer with each other with the number of fusion iterations carried out between them.

TABLE II
AVERAGE RMSE OF DIFFERENT FILTERS IN THE NONLINEAR SCENARIO

Filter	Position [m]	Velocity [m/s]	Turn-rate [deg/s]
Noncoop. CKF I	13.80	3.20	1.69
CKF-IC	11.94	2.97	1.66
CKF-NF	247.49	2 15.76	3.74
CKF-AA	12.42	3.10	1.66
CKF-CI	12.39	3.02	1.95
CKF-CU	18.47	4.53	1.84
Noncoop. SIR I	26.80	4.11	1.91
SIR-IC	44.40	4.49	2.29
SIR-NF	286.29	16.20	3.35
SIR-AA	12.54	3.13	1.71
SIR-CI	12.81	3.09	1.69
SIR-CU	18.43	4.18	1.88

V. CONCLUSION

In this paper, we present some statistic and information-theoretic results on the FMD given by linear density fusion, analyzing the covariance consistency, MSE, mode-preservation capacity of the AA fusion and its relationship with some existing fusion approaches including CU and CI. Principled, suboptimal methods are proposed for online determining the fusing weights of the AA fusion approach. Representative scenarios and simulations have been considered for verifying these theoretical findings which add to the theoretical base of this fundamental information fusion approach and may thereby promote its further development.

REFERENCES

- [1] X. Li, Y. Zhu, J. Wang, and C. Han, "Optimal linear estimation fusion. I. Unified fusion rules," *IEEE Transactions on Information Theory*, vol. 49, no. 9, pp. 2192–2208, 2003.
- [2] R. Olfati-Saber, J. A. Fax, and R. M. Murray, "Consensus and cooperation in networked multi-agent systems," *Proc. IEEE*, vol. 95, no. 1, pp. 215–233, Jan. 2007.
- [3] A. H. Sayed, "Adaptation, learning, and optimization over networks," *Found. Trends in Machine Learn.*, vol. 7, no. 4–5, pp. 311–801, 2014.
- [4] K. Da, T. Li, Y. Zhu, H. Fan, and Q. Fu, "Recent advances in multisensor multitarget tracking using random finite set," *Front Inform Technol Electron Eng.*, vol. 22, no. 1, pp. 5–24, 2021.
- [5] S. H. Javadi and A. Farina, "Radar networks: A review of features and challenges," *Information Fusion*, vol. 61, pp. 48–55, 2020.
- [6] T. Li, H. Fan, J. García, and J. M. Corchado, "Second-order statistics analysis and comparison between arithmetic and geometric average fusion: Application to multi-sensor target tracking," *Information Fusion*, vol. 51, pp. 233 – 243, 2019.
- [7] R. P. S. Mahler, *Advances in Statistical Multisource-Multitarget Information Fusion*, ser. Electronic Warfare. Artech House, 2014.
- [8] T. Li, J. Corchado, and S. Sun, "Partial consensus and conservative fusion of Gaussian mixtures for distributed PHD fusion," *IEEE Trans. Aerosp. Electron. Syst.*, vol. 55, no. 5, pp. 2150–2163, Oct. 2019.
- [9] T. Li and F. Hlawatsch, "A distributed particle-PHD filter using arithmetic-average fusion of Gaussian mixture parameters," *Information Fusion*, vol. 73, pp. 111–124, 2021, arXiv:1712.06128.
- [10] T. Li, Z. Liu, and Q. Pan, "Distributed Bernoulli filtering for target detection and tracking based on arithmetic average fusion," *IEEE Signal Proc. Lett.*, vol. 26, no. 12, pp. 1812–1816, Dec. 2019.
- [11] H. Kim, K. Granström, L. Gao, G. Battistelli, S. Kim, and H. Wymeersch, "5G mmwave cooperative positioning and mapping using multi-model PHD filter and map fusion," *IEEE Trans. Wireless Commun.*, vol. 19, no. 6, pp. 3782–3795, 2020.
- [12] R. K. Ramachandran, N. Fronda, and G. Sukhatme, "Resilience in multi-robot multi-target tracking with unknown number of targets through reconfiguration," *IEEE Trans. Contr. Netw. Syst.*, vol. 8, no. 2, pp. 609–620, 2021.

- [13] K. Da, T. Li, Y. Zhu, and Q. Fu, "Gaussian mixture particle jump-Markov-CPHD fusion for multitarget tracking using sensors with limited views," *IEEE Trans. Signal Inform. Process. Netw.*, vol. 6, pp. 605–616, Aug. 2020.
- [14] L. Gao, G. Battistelli, and L. Chisci, "Multiobject fusion with minimum information loss," *IEEE Signal Process. Lett.*, vol. 27, pp. 201–205, Jan. 2020.
- [15] T. Li, X. Wang, Y. Liang, and Q. Pan, "On arithmetic average fusion and its application for distributed multi-Bernoulli multitarget tracking," *IEEE Trans. Signal Process.*, vol. 68, pp. 2883–2896, 2020.
- [16] G. Li, G. Battistelli, L. Chisci, W. Yi, and L. Kong, "Distributed multi-view multi-target tracking based on CPHD filtering," *Signal Processing*, vol. 188, p. 108210, 2021.
- [17] S. Frühwirth-Schnatter, *Finite Mixture and Markov Switching Models*, ser. Springer Series in Statistics. NY: Springer New York, 2006.
- [18] T. M. Frago, W. Bertoli, and F. Louzada, "Bayesian model averaging: A systematic review and conceptual classification," *Int Stat Rev*, vol. 86, no. 1, pp. 1–28, 2018.
- [19] J. Zhang, Z. Yin, P. Chen, and S. Nichele, "Emotion recognition using multi-modal data and machine learning techniques: A tutorial and review," *Information Fusion*, vol. 59, pp. 103–126, 2020.
- [20] H. Cui, X. Wang, S. Gao, and T. Li, "A gaussian mixture regression model based adaptive filter for non-gaussian noise without a priori statistic," *Signal Processing*, vol. 190, p. 108314, 2022.
- [21] B.-N. Vo, M. Mallick, Y. Bar-shalom, S. Coraluppi, R. Osborne, R. Mahler, and B.-T. Vo, "Multitarget tracking," in *Wiley Encyclopedia of Electrical and Electronics Engineering*. John Wiley & Sons, 2015.
- [22] S. R. Dalal and W. J. Hall, "Approximating priors by mixtures of natural conjugate priors," *Journal of the Royal Statistical Society: Series B (Methodological)*, vol. 45, no. 2, pp. 278–286, 1983.
- [23] P. Diaconis and D. Ylvisaker, "Quantifying prior opinion," *Report Number: EFS NSF207*, Oct. 1983.
- [24] D. Peel and G. McLachlan, "Robust mixture modelling using the t distribution," *Stat. Comput.*, vol. 10, no. 4, pp. 339–348, 2000.
- [25] B.-T. Vo and B.-N. Vo, "Labeled random finite sets and multi-object conjugate priors," *IEEE Trans. Signal Process.*, vol. 61, no. 13, pp. 3460–3475, Jul. 2013.
- [26] A. F. García-Fernández, J. L. Williams, K. Granström, and L. Svensson, "Poisson multi-Bernoulli mixture filter: Direct derivation and implementation," *IEEE Trans. Aerosp. Electron. Syst.*, vol. 54, no. 4, pp. 1883–1901, 2018.
- [27] G. McLachlan and D. Peel, *Finite Mixture Models*, ser. Wiley Series in Probability and Statistics. New York, USA: Wiley, 2000.
- [28] S. M. Kay, *Fundamentals of Statistical Signal Processing: Estimation Theory*. Upper Saddle River, NJ, USA: Prentice-Hall, 1993.
- [29] X. Li, Y. Zhu, J. Wang, and C. Han, "Optimal linear estimation fusion. i. unified fusion rules," *IEEE Trans. Inform. Theory*, vol. 49, no. 9, pp. 2192–2208, 2003.
- [30] S.-L. Sun, "Distributed optimal linear fusion estimators," *Information Fusion*, vol. 63, pp. 56–73, 2020.
- [31] J. K. Uhlmann, "Dynamic map building and localization: New theoretical foundations," Ph.D. dissertation, University of Oxford, UK, 1995.
- [32] —, "Covariance consistency methods for fault-tolerant distributed data fusion," *Inf. Fusion*, vol. 4, no. 3, pp. 201–215, 2003.
- [33] S. J. Julier, "An empirical study into the use of chernoff information for robust, distributed fusion of Gaussian mixture models," in *Proc. FUSION 2006*, Florence, Italy, Jul. 2006.
- [34] O. Bochar, R. Calhoun, J. K. Uhlmann, and S. J. Julier, "Generalized information representation and compression using covariance union," in *Proc. FUSION 2006*, Florence, Italy, Jul. 2006.
- [35] X. R. Li and Z. Zhao, "Measuring estimator's credibility: Noncredibility index," in *Proc. FUSION 2006*, Florence, Italy, 2006, pp. 1–8.
- [36] J. Ajgl and M. Šimandl, "Conservativeness of estimates given by probability density functions: Formulation and aspects," *Inf. Fusion*, vol. 20, pp. 117–128, 2014.
- [37] S. Lubold and C. N. Taylor, "Formal definitions of conservative PDFs," [Online] *arXiv:1912.06780v2*, 2019.
- [38] S. J. Julier and J. K. Uhlmann, "Fusion of time delayed measurements with uncertain time delays," in *Proc. ACC 2005*, Portland, OR, USA, Jun. 2005, pp. 4028–4033.
- [39] X. Wang, S. Sun, T. Li, and Y. Liu, "Fault tolerant multi-robot cooperative localization based on covariance union," *IEEE Robotics and Automation Letters*, vol. 6, no. 4, pp. 7799–7806, 2021.
- [40] D. J. Salmond, "Mixture reduction algorithms for point and extended object tracking in clutter," *IEEE Trans. Aerosp. Electron. Syst.*, vol. 45, no. 2, pp. 667–686, 2009.
- [41] A. R. Runnalls, "Kullback-Leibler approach to Gaussian mixture reduction," *IEEE Trans. Aerosp. Electron. Syst.*, vol. 43, no. 3, pp. 989–999, July 2007.
- [42] S. Julier and J. Uhlmann, "General decentralized data fusion with covariance intersection (CI)," in *Handbook of Data Fusion*, D. Hall and J. Llinas, Eds. Boca Raton, FL, USA: CRC Press, 2001, ch. 12, pp. 1–25.
- [43] S. Reece and S. Roberts, "Robust, low-bandwidth, multi-vehicle mapping," in *Proc. FUSION 2005*, vol. 2, Philadelphia, PA, USA, 2005.
- [44] J. Sijs and M. Lazar, "State fusion with unknown correlation: Ellipsoidal intersection," *Automatica*, vol. 48, no. 8, pp. 1874–1878, 2012.
- [45] B. Noack, J. Sijs, M. Reinhardt, and U. D. Hanebeck, "Decentralized data fusion with inverse covariance intersection," *Automatica*, vol. 79, pp. 35–41, 2017.
- [46] Y. Wang and X. R. Li, "A fast and fault-tolerant convex combination fusion algorithm under unknown cross-correlation," in *Proc. FUSION 2009*, Seattle, Washington, USA, Jul. 2009, pp. 571–578.
- [47] R. P. S. Mahler, "The multisensor PHD filter: II. Erroneous solution via Poisson magic," in *Proc. SPIE*, vol. 7336, 2009, pp. 7336–12.
- [48] S. Sarkka and A. Nummenmaa, "Recursive noise adaptive Kalman filtering by variational Bayesian approximations," *IEEE Trans. Autom. Contr.*, vol. 54, no. 3, pp. 596–600, 2009.
- [49] B.-T. Vo, B.-N. Vo, R. Hoseinnezhad, and R. P. S. Mahler, "Robust multi-Bernoulli filtering," *IEEE J. Sel. Topics Signal Process.*, vol. 7, no. 3, pp. 399–409, 2013.
- [50] T. Li, S. Rodríguez, J. Bajo, J. M. Corchado, and S. Sun, "On the bias of the SIR filter in parameter estimation of the dynamics process of state space models," in *Proc. DCAI'15*, Salamanca, Spain, 2015, pp. 87–95.
- [51] A. E. Abbas, "A Kullback-Leibler view of linear and log-linear pools," *Decision Analysis*, vol. 6, no. 1, pp. 25–37, 2009.
- [52] K. Da, T. Li, Y. Zhu, H. Fan, and Q. Fu, "Kullback-Leibler averaging for multitarget density fusion," in *Proc. DCAI 2019*, Avila, Spain, Jun. 2019, pp. 253–261.
- [53] T. Ardeshiri, U. Orguner, and E. Özkan, "Gaussian mixture reduction using reverse Kullback-Leibler divergence," 2015, arxiv.org/abs/1508.05514.
- [54] R. E. Blahut, *Principles and Practice of Information Theory*. USA: Addison-Wesley Longman Publishing Co., Inc., 1987.
- [55] T. M. Cover and J. A. Thomas, *Elements of Information Theory*. John Wiley & Sons, Ltd, 2001.
- [56] F. Nielsen, "An information-geometric characterization of Chernoff information," *IEEE Signal Proc. Lett.*, vol. 20, no. 3, pp. 269–272, 2013.
- [57] M. Üney, J. Houssineau, E. Delande, S. J. Julier, and D. E. Clark, "Fusion of finite set distributions: Pointwise consistency and global cardinality," *IEEE Trans. Aerosp. Electron. Syst.*, vol. 55, no. 6, pp. 2759–2773, 2019.
- [58] M. B. Hurley, "An information theoretic justification for covariance intersection and its generalization," in *Proc. FUSION 2002*, Annapolis, MD, USA, Jul. 2002, pp. 505–511.
- [59] N. R. Ahmed and M. Campbell, "Fast consistent Chernoff fusion of Gaussian mixtures for ad hoc sensor networks," *IEEE Trans. Signal Process.*, vol. 60, no. 12, pp. 6739–6745, 2012.
- [60] N. R. Ahmed, J. R. Schoenberg, and M. E. Campbell, *Fast Weighted Exponential Product Rules for Robust General Multi-Robot Data Fusion*. MIT Press, 2013, pp. 9–16.
- [61] J. R. Hershey and P. A. Olsen, "Approximating the Kullback Leibler divergence between Gaussian mixture models," in *Proc. ICASSP '07*, vol. 4, 2007, pp. 317–320.
- [62] N. Bouhlef and A. Dziri, "Kullback-Leibler divergence between multivariate generalized Gaussian distributions," *IEEE Signal Proc. Lett.*, vol. 26, no. 7, pp. 1021–1025, 2019.
- [63] M. Fontana, A. F. Garcia-Fenandez, and S. Maskell, "Bernoulli merging for the poisson multi-bernoulli mixture filter," in *Proc. FUSION 2020*, Rustenburg, South Africa, 2020, pp. 1–8.
- [64] S. Matzka and R. Altendorfer, "A comparison of track-to-track fusion algorithms for automotive sensor fusion," in *Proc. MFI 2008*, 2008, pp. 189–194.
- [65] B. Noack, U. Orguner, and U. D. Hanebeck, "Nonlinear decentralized data fusion with generalized inverse covariance intersection," in *Proc. FUSION 2019*, Ottawa, ON, Canada, 2019.
- [66] I. Arasaratnam and S. Haykin, "Cubature Kalman filters," *IEEE Trans. Autom. Control*, vol. 54, no. 6, pp. 1254–1269, June 2009.
- [67] T. Li, M. Bolić, and P. M. Djurić, "Resampling methods for particle filtering: Classification, implementation, and strategies," *IEEE Signal Process. Mag.*, vol. 32, no. 3, pp. 70–86, May 2015.